ACS APPLIED MATERIALS & INTERFACES

Research Article

www.acsami.org

High-Performance Multilayer Composite Membranes with Mussel-Inspired Polydopamine as a Versatile Molecular Bridge for CO_2 Separation

Panyuan Li, Zhi Wang,* Wen Li, Yanni Liu, Jixiao Wang, and Shichang Wang

Chemical Engineering Research Center, School of Chemical Engineering and Technology, Tianjin University, Tianjin 30072, PR China

Tianjin Key Laboratory of Membrane Science and Desalination Technology, State Key Laboratory of Chemical Engineering, Collaborative Innovation Center of Chemical Science and Engineering (Tianjin), Tianjin University, Tianjin 30072, PR China

Supporting Information

ABSTRACT: It is desirable to develop high-performance composite membranes for efficient CO_2 separation in CO_2 capture process. Introduction of a highly permeable polydimethylsiloxane (PDMS) intermediate layer between a selective layer and a porous support has been considered as a simple but efficient way to enhance gas permeance while maintaining high gas selectivity, because the introduced intermediate layer could benefit the formation of an ultrathin defect-free selective layer owing to the circumvention of pore penetration phenomenon. However, the selection of selective layer materials is unfavorably restricted because of the low surface energy of PDMS. Various highly hydrophilic membrane materials such as amino group-rich polyvinylamine (PVAm), a representative facilitated transport membrane material for CO_2 separation, could not be facilely coated over the surface of the hydrophobic PDMS intermediate layer uniformly. Inspired by the hydrophilic nature and strong adhesive ability of polydopamine (PDA), PDA was therefore selected as a versatile molecular bridge between hydrophobic PDMS and hydrophilic PVAm. The PDA coating endows a highly compatible interface between both components with a large surface energy difference via multiple-site cooperative interactions. The resulting multilayer composite membrane with a thin facilitated transport PVAm selective layer exhibits a notably enhanced CO_2 permeance (1887 GPU) combined with a slightly improved CO_2/N_2 selectivity (83), as well as superior structural stability. Similarly, the multilayer composite membrane with a hydrophilic CO_2-philic Pebax 1657 selective layer was also developed for enhanced CO_2 separation performance.

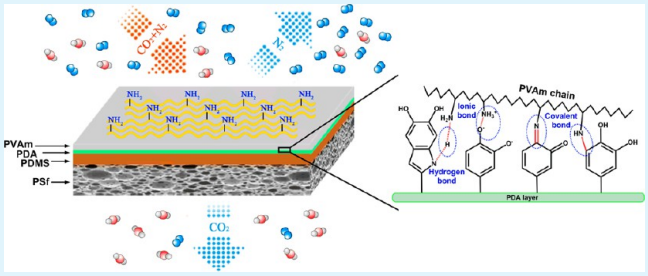

KEYWORDS: *composite membrane, intermediate layer, gas separation, polydopamine, polyvinylamine*

1. INTRODUCTION

Membrane-based gas separation technology has attracted considerable attention in both scientific and industrial communities because of its potential application in energy and environmental related fields.[1−3] Attributed to the distinct advantages of environmental compatibility, energy efficiency, and small footprint, membrane-based gas separation technology has been commercially used in air separation, natural gas sweeting and hydrogen recovery from purge gases or refinery gases.[4,5] So far, it is however challenging for commercial membranes to meet the requirements for some large-scale applications such as postcombustion CO_2 capture. High-performance membranes are therefore urgently required in order to strengthen the technological and economic competitiveness of membrane process.[6−8] High permeance is generally even more favorable than high selectivity due to the limitation of affordable pressure ratio (5−15) in terms of postcombustion CO_2 capture.[9] Hence, a membrane with a high CO_2 permeance (>1000 GPU; 1 GPU = 10^{-6} m^3 (STP) m^{-2} s^{-1} $cmHg^{-1}$) accompanied by a moderate CO_2/N_2 selectivity (∼30), has been extensively considered necessary to compete with absorption process.[10]

Nowadays, the overwhelming strategy toward membranes with a high permeance is to develop high permeability membrane materials, such as thermally rearranged (TR) polymers, polymers of intrinsic microporosity (PIMs), and metal organic frameworks (MOFs).[11−13] It is worth noting that a high permeability of membrane materials does not necessarily mean a high permeance of the resulting membranes. In fact, the permeance of a membrane is closely related to its thickness besides intrinsic gas transport properties of membrane materials. Therefore, the membrane should be as thin as possible without forming defects for obtaining a sufficiently high permeance while maintaining a favorable selectivity. As a

Received: May 1, 2015
Accepted: June 29, 2015
Published: June 29, 2015

DOI: 10.1021/acsami.5b03786
ACS Appl. Mater. Interfaces 2015, 7, 15481−15493

Scheme 1. Schematic Illustration of the PVAm/PDA−PDMS/PSf Multilayer Composite Membranes with a Highly Compatibility Interface through the Mediation of Polydopamine

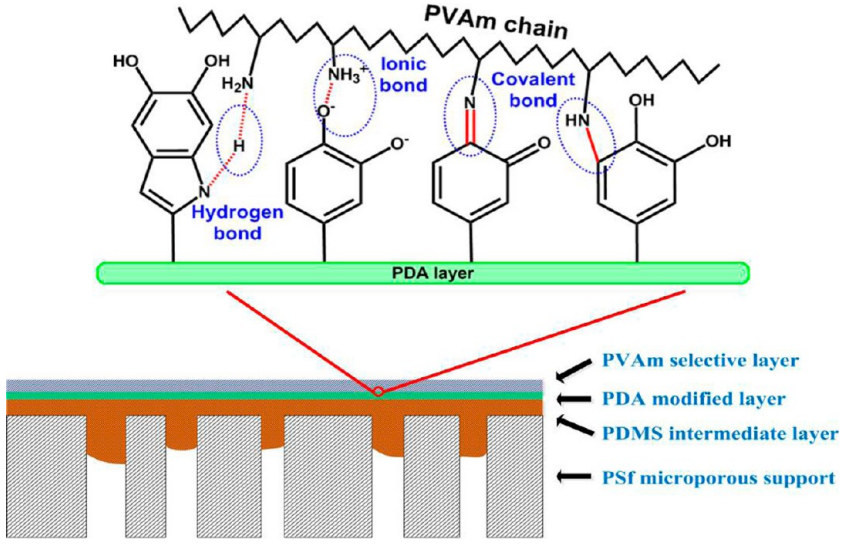

consequence, only if a membrane material can be processed into a thin defect-free selective layer on a porous support or an asymmetric membrane with enough mechanical strength, it would be economically competitive.[14] Unfortunately, the unfavorable solution processable property of some aforementioned materials possessing high gas permeability restricts the fabrication of thin film composite (TFC) membranes.[15] Furthermore, it is still a challenging issue to develop a perfect thin layer even for soluble materials.[16] Accordingly, the development of advanced membrane materials and corresponding thin membrane fabrication techniques should be simultaneously conducted for fabricating membranes with high permeance and high selectivity.

Coating is one of the most common processes of manufacturing thin films as membranes on large scale, which mainly includes dip-coating, spraying-coating, and blade-coating. For the blade-coating process, decreasing wet coating thickness and diluting coating solution are two primary strategies to obtain a thin solid selective layer. Compared with decreasing wet coating thickness, diluting coating solution generally shows the advantages of operational simplicity and good reproducibility which are vital for large-scale production. However, the coating solution with a lower concentration could penetrate into the pores of porous supports, namely the so-called pore penetration phenomenon. This phenomenon may result in the generation of defects in the selective layer.[17] In addition, pore penetration phenomenon could possibly bring about a substantial increase in effective selective layer thickness, according to the classical model about gas transport behavior of composite membranes that total resistance increases linearly with intruded depth in most cases.[18−20] Both of them could cause an obvious deterioration of membrane performances. To address this problem, introduction of a pore-free intermediate layer between the porous support and the selective layer is a widely adopted strategy.[21−23] In addition, the intermediate layer could optimize the gas flow distribution and enhance the utilization efficiency of selective layer.[24] A desirable intermediate layer is expected to be as permeable as possible to minimize the contribution to total gas transport resistance. Meanwhile, the intermediate layer should have a good compatibility with the porous support, as well as the selective layer, ensuring the membrane with a favorable structural stability. Currently, the most conventional membrane material for intermediate layer is polydimethylsiloxane (PDMS). For example, the commercial Polaris polymeric membrane manufactured by Membrane Technology and Research Inc. (MTR), includes a highly permeable PDMS intermediate layer.[25]

It should be noted that the cross-linked PDMS intermediate layer is generally hydrophobic, restricting the selection of materials as selective layers. Many superior membrane materials for CO_2 separation, such as amino group-rich polymers for facilitated transport membranes and ethylene oxide (EO) group-rich polymers for CO_2-philic polymeric membranes, are highly hydrophilic or even water-soluble, it is therefore difficult for their corresponding solutions to spread uniformly over the surface of the hydrophobic PDMS intermediate layer and subsequently to form an intact defect-free selective layer when environmental-friendly water-based solvents are used. To render these membrane materials facilely deposit on the PDMS intermediate layer, surface hydrophilic modification of PDMS intermediate layer is necessary. In addition, PDMS generally shows the poor adhesion to other materials.[26] Hence, there exists a potential instability between PDMS intermediate layer and selective layer during long-term operation, and it is essential to construct a robust and compatible interface between layers for improving the structural stability of multilayer composite membranes.

Inspired by a biological adhesive protein of marine mussels, many researches have demonstrated that polydopamine (PDA) can conveniently deposit and further adhere on virtually all types of inorganic and organic supports, with controllable film thickness and durable stability via the oxidative self-polymerization of dopamine (DOP) in a mildly alkaline environment. The widely accepted reasons for this unique adhesion characteristic are the catechol structure with strong adhesion and the formed cross-linked network via autoxidation.[27,28] Owing to the universal adhesive property, surface coating with PDA has become a popular approach to improving the hydrophilic property of material surface along with the hydrophilic nature of PDA.[29,30] In addition, PDA coating provides a versatile platform for postfunctionalization, such as

DOI: 10.1021/acsami.5b03786
ACS Appl. Mater. Interfaces 2015, 7, 15481−15493

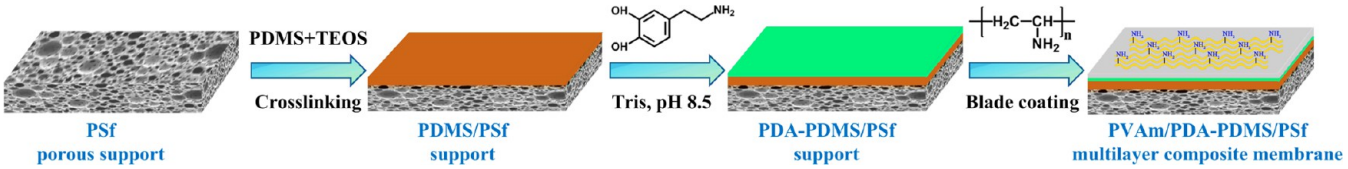

Figure 1. Schematic diagram of the preparation of the PVAm/PDA−PDMS/PSf multilayer composite membranes.

metal deposition and covalent immobilization of nucleophilic species, because it possesses abundant functional groups including amino group and catechol group.[31−33] Accordingly, mussel-inspired surface chemistry based on PDA coating has opened a new route to material modification owing to its extensive applicability, simplicity, and versatility.[34]

In the present work, PDA was selected to modify surface properties of the PDMS intermediate layer for promoting the homogeneous deposition of water-soluble polyvinylamine (PVAm), which is the representative facilitated transport membrane material for CO_2 separation. There are the following four aspects to endow the favorable compatibility between the intermediate layer and the selective layer and further promote the formation of a thin defect-free PVAm selective layer (Scheme 1). First, the introduced hydrophilic groups from PDA render the PDA-decorated PDMS intermediate layer improved water wettability compared to the pristine PDMS intermediate layer, which benefits the uniform spread of PVAm aqueous solution over the surface of the intermediate layer. Second, there exist numerous hydrogen bonds between polar groups on PDA and PVAm to improve the compatibility. Third, PVAm shows the cationic character in the aqueous solution owing to the protonation of primary amino groups, meanwhile, PDA is directed toward a negative charge because of the deprotonation of catechol groups when immersed in a mildly basic solution environment.[35] Therefore, positively charged PVAm molecules could readily absorb onto the surface of negatively charged PDA-decorated PDMS intermediate layer through electrostatic attraction. Last but not the least, catechol groups or quinone groups of PDA could react with primary amino groups of PVAm via Michael addition or Schiff base reaction under weakly alkaline conditions, rendering the covalent linkage on the interface between PDA-decorated PDMS intermediate layer and PVAm selective layer. As a consequence, high-performance structurally stable PVAm/PDA−PDMS/polysulfone (PSf) multilayer composite membranes were successfully developed via the mediation of PDA as a versatile molecular bridge, which consist of a PSf porous support, a PDA-decorated cross-linked PDMS intermediate layer and a thin PVAm selective layer. Compared to that without PDA-decorated PDMS intermediate layer, the as-developed multilayer composite membrane exhibits a dramatically higher CO_2 permeance along with a favorable CO_2/N_2 selectivity owing to an ultrathin defect-free selective layer. This work may provide a universal strategy to develop high-performance composite membranes where a thin hydrophilic selective layer is coated on a hydrophobic support.

2. EXPERIMENTAL SECTION

2.1. Materials. The polysulfone ultrafiltration flat sheet membranes were purchased from Vontron Technology Co., Ltd., (China) as porous supports. Polydimethylsiloxane (PDMS) was provided from ShinEtsu (Japan). Tetraethoxysilane (TEOS, 99.99 wt %), di-tin butyl dilaurate (DBD, 95 wt %), dopamine hydrochloride (DOP·HCl, 98 wt %), and tris(hydroxymethyl)aminomethane (Tris, 99.5 wt %) were supplied by Aladdin Reagent CO. Ltd. (China). *N*-Vinylformamide (NVF, 98%) and 2,2′-azobis(2-methylpropionamidine) dihydrochloride (AIBA, 97 wt %) were purchased from Sigma-Aldrich (China). Pebax 1657 (containing 60 wt % polyether segments and 40 wt % polyamide segments) was purchased from Arkema (France). All the other reagents were of analytical grade and used without further purification.

2.2. Fabrication of Supports. *2.2.1. PDMS/PSf Support.* The partially cross-linked PDMS solution was prepared by dissolving 0.5 wt % PDMS, 0.4 wt % TEOS as cross-linker and 0.4 wt % DBD as catalyst in heptane, followed by vigorously stirring for 30 min at room temperature. Before use, the partially cross-linked PDMS solution was stored in an ice bath to inhibit further cross-linking reaction. The solution was coated on top of the PSf porous supports with the wet coating thickness of about 100 μm using a homemade applicator, and then the support was kept at 303 K and 40% relative humidity in an artificial climate chamber (Climacell 222R, Germany) for at least 12 h to allow further cross-linking reaction.

2.2.2. PDA−PDMS/PSf Supports. The dopamine solution was prepared by dissolving dopamine hydrochloride at a concentration of 2.0 mg/mL in Tris butter solution (50 mM, pH 8.5). The as-prepared PDMS/PSf support was first clamped between two Teflon frames, and then the DOP solution was poured onto the surface of the PDMS side of the PDMS/PSf support. Last, the PDMS/PSf support was shaken in an open vessel at 303 K for a scheduled time (5−20 min). After that, the support was taken out and washed repeatedly with deionized water and ethanol alternatively to remove unattached and weakly bound PDA from the support surface. It should be noted that the PDA deposition only occurs on the PDMS side because there is no DOP solution on the PSf side. The resulting PDA−PDMS/PSf support was stored under humid conditions prior to use.

2.3. Fabrication of Multilayer Composite Membranes. *2.3.1. PVAm/PDA−PDMS/PSf Multilayer Composite Membranes.* PVAm was synthesized via free radical polymerization of NVF and subsequently acid hydrolysis and ion exchange treatment (Scheme S1 in Supporting Information), as described in our previous study.[36] PVAm was dissolved into deionized water to obtain a homogeneous coating solution at room temperature. The concentration of PVAm aqueous solutions ranged from 0.3 to 1.0 wt %. PVAm/PDA−PDMS/PSf multilayer composite membranes were prepared by casting PVAm aqueous solutions with different concentrations on top of the PDA−PDMS/PSf supports with the wet coating thickness of about 100 μm and then dried at 303 K and 40% relative humidity for at least 12 h. The schematic diagram of the preparation of the PVAm/PDA−PDMS/PSf multilayer composite membranes is illustrated in Figure 1. The resulting membranes were denoted as PVAm(x)/PDA(y)-PDMS/PSf membranes, where x represents the concentration of PVAm solution, and y means the deposition time of dopamine. For comparison, PVAm/PSf membranes were also prepared under the same conditions.

2.3.2. Pebax 1657/PDA−PDMS/PSf Multilayer Composite Membranes. Pebax 1657 solutions were prepared by dissolving Pebax 1657 into ethanol/water (70/30 wt %) mixed solvent with stirring and reflux at 353 K. Similarly, Pebax 1657/PDA−PDMS/PSf membranes and Pebax 1657/PSf membranes were fabricated via solution coating method described above.

2.4. Membrane Characterization. The surface morphology and cross-sectional structure of the supports and membranes were characterized by scanning electron microscopy (SEM, Nova Nano430, FEI of USA). For the cross-sectional observation, the samples were prepared by peeling away the polyester backing fabric,

DOI: 10.1021/acsami.5b03786
ACS Appl. Mater. Interfaces 2015, 7, 15481−15493

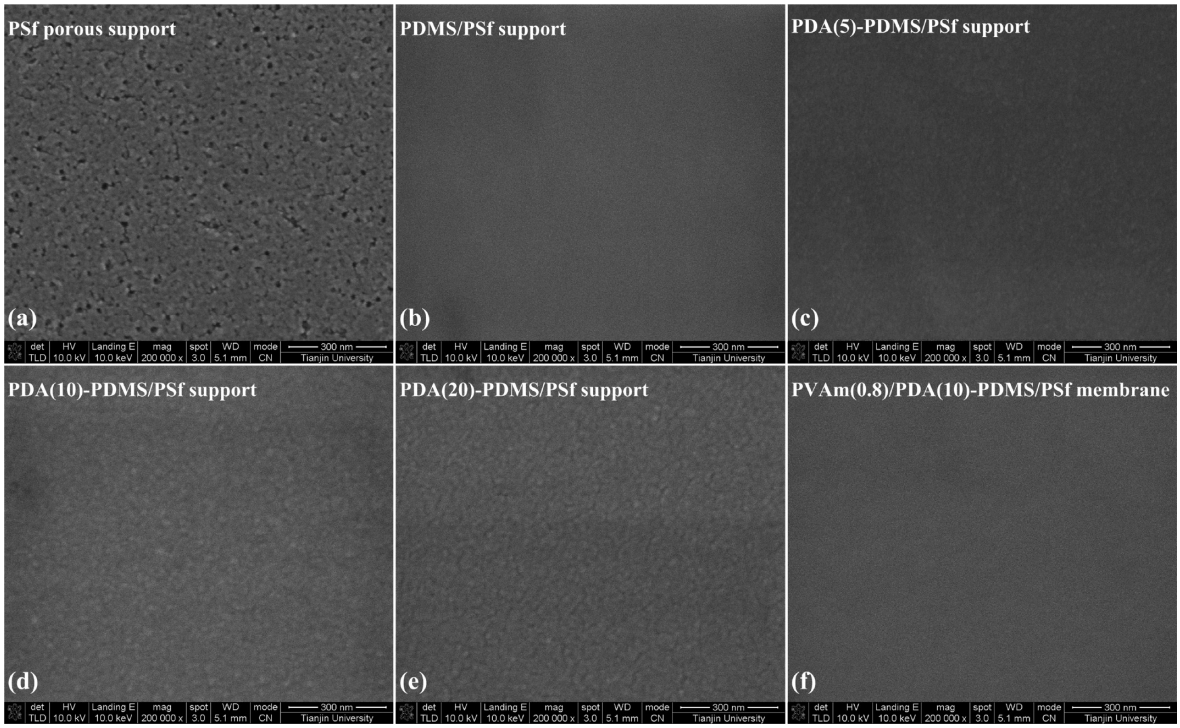

Figure 2. Surface SEM images of the supports and membrane: (a) PSf porous support, (b) PDMS/PSf support, (c) PDA(5)-PDMS/PSf support, (d) PDA(10)-PDMS/PSf support, (e) PDA(20)-PDMS/PSf support, and (f) PVAm(0.8)/PDA(10)-PDMS/PSf membrane. Scale bar: 300 nm.

and then freeze-fractured in liquid nitrogen. All samples were coated with gold by a sputter-coating machine before SEM analysis. The average pore size of the commercial PSf porous support used was determined by the analysis of surface SEM image using ImageJ software.[37] The layer thickness obtained from SEM images was averaged from at least three locations of one membrane sample.

Attenuated total reflectance infrared (ATR-FTIR) spectroscopy (FTS-6000, Bio-Rad of USA), X-ray photoelectron spectroscopy (XPS, PHI-1600) and Raman spectroscopy (DXR Raman Spectrometer of Thermo Fisher Scientific) were used to investigate the chemical structure and chemical composition of the supports and membranes. ATR-FTIR analysis was performed with a resolution of 4 cm^{-1} in the range of 400−4000 cm^{-1} at room temperature. XPS analysis was performed using Al Kα (1486.6 eV) as the radiation source and the spectra were taken with the electron emission angle at 90° with respect to the sample surface. Raman analysis was conducted with Nd:YAG laser (532 nm) as an excitation source.

The static water contact angles of the supports were measured via a contact angle goniometer (OCA15EC, Dataphysics, Germany) under ambient conditions at room temperature. A water droplet with the volume of 2 μL was dropped on the sample surface with a microsyringe. At least five water contact angles at different locations on one sample surface were averaged to obtain a reliable value.

2.5. Gas Permeation Measurements. Gas permeation measurements were conducted at 298 K with conventional constant pressure/variable volume method using the homemade gas permeation apparatus (Figure S1 in Supporting Information). The membrane with effective membrane area of 19.26 cm^2 was mounted in a circular stainless steel cell. Both the feed gas and the sweep gas (H_2) were saturated with water vapor by passing through a water bottle prior to contacting the membrane. The upstream pressure varied from 0.15 to 2.00 MPa, while the downstream pressure in the apparatus was maintained at atmosphere pressure. The steady state permeation was assumed to have been reached when the outlet sweep gas flow rate and its composition no longer changed with time. The flow rate of the outlet sweep gas was obtained by a soap film flow meter, and the composition was analyzed by a gas chromatograph (HP 7890A) equipped with a thermal conductivity detector. In the current work, the membrane stage cut was below 1%, therefore, the permeance and selectivity for binary gas mixtures were calculated from the outlet sweep gas flow rate and the composition of permeate side. The permeance is defined as the flux divided by the partial pressure difference between the upstream and downstream side, and it is expressed in the unit of GPU. The selectivity is given by the ratio of permeances of CO_2 over N_2. All error bars represent the standard errors of the performances of three samples prepared and tested under the same conditions. In addition, it should be mentioned that effects of back-diffusion of the sweep gas and concentration polarization on data analysis could be neglected based on our previous study.[38,39]

2.6. Structural Stability Tests. The structural stability of the PVAm/PDA−PDMS/PSf multilayer composite membranes was investigated by hexane treatment and continuous gas permeation test under humid conditions. The multilayer composite membrane was first immersed in hexane for 24 h to render PDMS fully swollen, and then the membrane was transferred to artificial climate chamber to let remaining hexane evaporate completely. The comparison of membrane separation performance before and after hexane treatment was conducted to examine the structural stability. Moreover, a 100-h continuous gas permeation test was carried out using humid feed gas to further investigate the structural stability.

3. RESULTS AND DISCUSSION

3.1. Surface Morphology and Chemical Composition of Supports and Membrane. The surface morphology of the PSf, PDMS/PSf, PDA−PDMS/PSf supports and PVAm/PDA−PDMS/PSf membrane are observed with SEM shown in Figure 2. The average pore size of the commercial PSf porous support used is about 10 nm from Figure 2a. The PDMS/PSf support possesses a very smooth surface (Figure 2b). Meanwhile, there is no visible pore from the surface SEM image. Compared to the pristine PDMS/PSf support, there is no much difference in surface morphology after surface modification using PDA due to the relatively short PDA deposition time. The surface of PDA−PDMS/PSf supports merely becomes a little rougher with increasing PDA

DOI: 10.1021/acsami.5b03786
ACS Appl. Mater. Interfaces 2015, 7, 15481−15493

deposition time, in contrast with that of the PDMS/PSf support. After PVAm coating, the membrane surface returns to be smooth similar to the PDMS/PSf support, and there is no defect or pinhole observed, which preliminarily reveals that PVAm is uniformly coated on the surface of the PDA-decorated PDMS intermediate layer.

The surface chemical structure of the PSf, PDMS/PSf, and PDA−PDMS/PSf supports as well as PVAm/PDA−PDMS/PSf membrane was investigated by ATR-FTIR, and the spectra are presented in Figure 3. Compared with that of the pristine

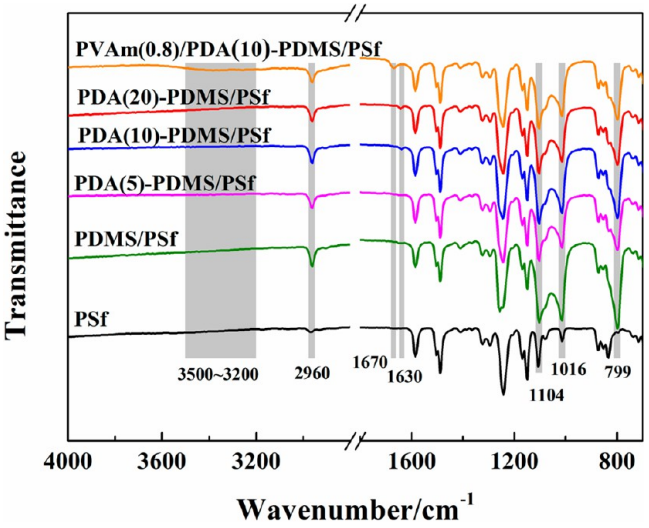

Figure 3. ATR-FTIR spectra of the PSf, PDMS/PSf and PDA−PDMS/PSf supports, as well as PVAm/PDA−PDMS/PSf membrane.

PSf porous support, a new strong peak at 799 cm^{-1} attributed to Si−O stretching vibration is observed.[40] Moreover, the relative intensity of the characteristic peaks at 2960, 1104, and 1016 cm^{-1}, increases significantly in the spectrum of the PDMS/PSf support. These peaks correspond to C−H stretching vibration of Si−CH_3 and Si−O−Si stretching vibration, respectively.[41] The spectra of PDA−PDMS/PSf supports are very similar to that of the PDMS/PSf support, except that there is an additional small peak at about 1630 cm^{-1} attributed to C═C stretching vibration in aromatic ring from PDA, confirming that PDA layer is successfully deposited on top of the PDMS/PSf support. Compared with that of PDA deposition (Figure S2 in Supporting Information), the intensity of characteristic peaks of PDA here is quite weak and even could not be detected, especially for polar groups of PDA. It is probably due to the following two reasons. On one hand, the thickness of the developed PDA layer (about a few nanometers) within such a short deposition time is much smaller than the detected depth of ATR-FTIR technique (about 500−1000 nm).[42,43] On the other hand, the potential hydrogen bond interaction between PDMS and PDA could render the intensity of peaks attributed to polar functional groups weaker.[44] Hence, this result implies the existence of hydrogen bond interaction between PDMS and PDA. After PVAm deposition, there appears a wide new peak at 3500−3200 cm^{-1} assigned to N−H stretching vibration, even if its relative intensity is very weak compared with that of PVAm bulk (Figure S3 in Supporting Information). This indicates hydrogen bond interaction between amino group of PVAm and amino groups of PDA. Moreover, another new peak at 1670 cm^{-1} is observed in the spectrum of the PVAm(0.8)/PDA(10)-PDMS/PSf membrane, which is in correspondence with C═O stretching vibration of residual amide group during PVAm synthesis.[36] Overall, the ATR-FTIR analysis also demonstrates that PVAm was successfully coated on top of the PDA−PDMS/PSf support. Moreover, it suggests hydrogen bond interaction between PDMS and PDA as well as between PDA and PVAm.

To investigate the chemical composition of different supports and membrane quantitatively, XPS analysis was adopted and the results are illustrated in Figure 4 and Table 1. It is expected

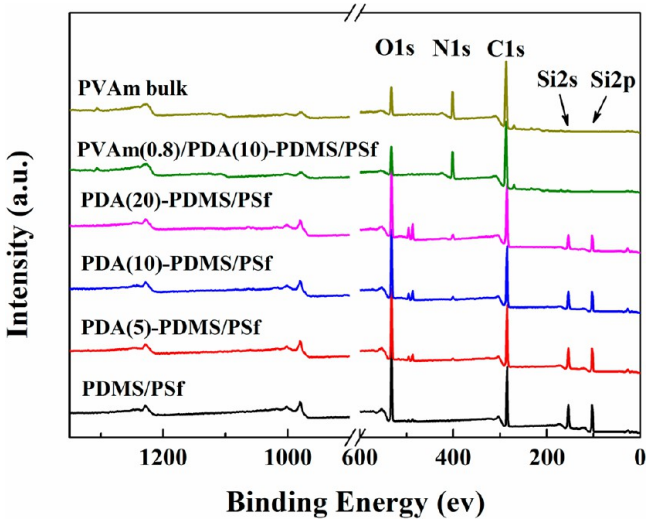

Figure 4. XPS spectra of the PDMS/PSf, PDA−PDMS/PSf supports, PVAm/PDA−PDMS/PSf membrane, and PVAm bulk sample.

Table 1. Surface Elemental Composition of the PDMS/PSf, PDA−PDMS/PSf Supports, PVAm/PDA−PDMS/PSf Membrane, and PVAm Bulk Sample

	surface elemental composition (at%)			
sample	C	O	N	Si
PDMS/PSf	49.06	26.01	-	24.93
PDA(5)−PDMS/PSf	51.82	25.23	1.45	21.50
PDA(10)−PDMS/PSf	54.42	24.76	2.22	18.60
PDA(20)−PDMS/PSf	58.24	23.69	3.56	14.50
PVAm(0.8)/PDA(10)−PDMS/PSf	70.27	10.03	19.41	0.29
PVAm bulk	70.13	10.23	19.64	

that the PDMS/PSf support possesses characteristic peaks of O 1s, C 1s, Si 2s, and Si 2p. Different from the pristine PDMS/PSf support, a new obvious peak of N 1s is observed in the PDA−PDMS/PSf supports, which is attributed to the nitrogen element of PDA. Moreover, the surface atomic percentage of nitrogen increases gradually with increasing PDA deposition time, meanwhile, the surface atomic percentage of silicon declines from 24.93% of the PDMS/PSf support to 14.50% of the PDA(20)−PDMS/PSf support, which suggests that an increasing amount of PDA is deposited on the PDMS/PSf support. Moreover, XPS results imply that the thickness of the formed PDA layer is smaller than the detection depth of XPS analysis (approximately 10 nm) owing to the existence of silicon for PDA−PDMS/PSf supports. A significant increase in surface nitrogen content is shown for the PVAm(0.8)/PDA(10)−PDMS/PSf membrane in comparison with the PDA−PDMS/PSf supports. The surface atomic percentage of

DOI: 10.1021/acsami.5b03786
ACS Appl. Mater. Interfaces 2015, 7, 15481−15493

silicon from PDMS underlying layer is merely 0.29% for the PVAm(0.8)/PDA(10)−PDMS/PSf membrane, furthermore the surface composition of the membrane almost coincides with that of PVAm bulk sample, indicating the perfect coverage of the PVAm selective layer onto the PDA(10)−PDMS/PSf support. Therefore, XPS analysis further demonstrates that the successful coating of the hydrophilic PVAm selective layer on top of the hydrophobic PDMS intermediate layer was achieved via surface modification of the PDMS intermediate layer using PDA. Furthermore, the core level XPS analysis of nitrogen and oxygen element of the PDA(10)−PDMS/PSf support and nitrogen element of the PVAm(0.8)/PDA(10)−PDMS/PSf membrane was investigated to explain the bonding mechanism of PDA layer and PVAm layer (Figure S4 and Figure S5 in Supporting Information). The results indicate the existence of quinone group and catechol group of PDA as well as the existence of primary amino group of PVAm. Accordingly, it could infer that Schiff base or Michael addition reaction could occur between PDA and PVAm. Moreover, the existence of corresponding functional groups also suggests that there is electrostatic attraction between the protonated amino groups of PVAm and deprotonated catechol groups of PDA during the deposition of PVAm aqueous solution. Unfortunately, the chemical structure of interface zone, the direct evidence of above bonding mechanism, could not be given, because the thickness of the developed PVAm layer is much larger than detection depth of XPS analysis.

Raman spectroscopy was used to further demonstrate the bonding mechanism of PDA and PVAm. Unfortunately, the characteristic peaks belonging to PDA and PVAm are too small to be detected from the spectra of PDA(10)-PDMS/PSf support and PVAm(0.8)/PDA(10)−PDMS/PSf membrane (Figure S6 in Supporting Information). Therefore, the PDA@PVAm complex was prepared to investigate the bonding mechanism between PDA and PVAm, which could circumvent the influence of the PSf support. As shown in Figure 5, two obvious peaks at 1356 and 1585 cm^{-1} assigned to the deformation of catechol group are observed in the spectrum of PDA.[30] The intensity of two peaks decreases notably after PVAm modification, suggesting the successful functionalization of PVAm onto PDA deposition. Moreover, the weakened intensity of peaks attributed to catechol group indicates the decreased content of catechol group owing to Schiff base or Michael addition reaction with amino group of PVAm, implying the presence of covalent bond between PDA and PVAm.

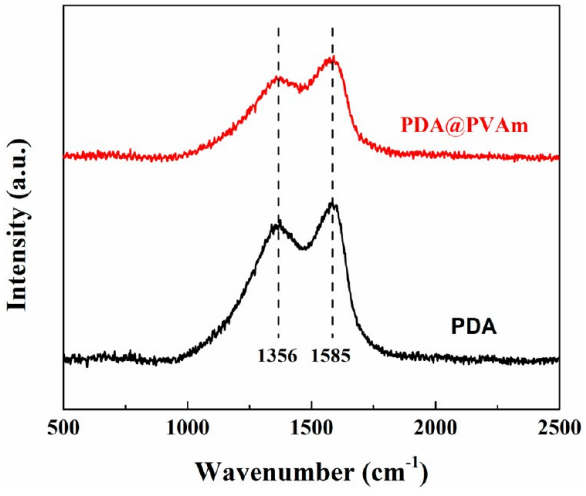

Figure 5. Raman spectra of PDA deposition and PDA@PVAm complex.

3.2. Surface Water Wettability of Supports. The water wettability of the PSf, PDMS/PSf, PDA−PDMS/PSf supports was evaluated by static water contact angle measurement. Figure 6 presents the water contact angle measured on the surface of different supports. As reported elsewhere, the water contact angle of the pristine PDMS/PSf support is around 107.7°, indicating the hydrophobic nature of PDMS.[45] Clearly, the water contact angles of the PDA−PDMS/PSf supports are obviously smaller than the pristine PDMS/PSf support, which indicates that PDA coating endows the surface of supports with enhanced water wettability owing to the hydrophilic nature of PDA. Moreover, the water contact angle gradually decreases with increasing PDA deposition time, and it declines to 69.8° and 50.4° at the deposition time of 10 and 20 min, respectively. These values are similar to that of the PSf porous support (~66.9°). It could be inferred that PVAm aqueous solution could spread well over the surface of the PDA-decorated PDMS intermediate layers with enough PDA deposition time.

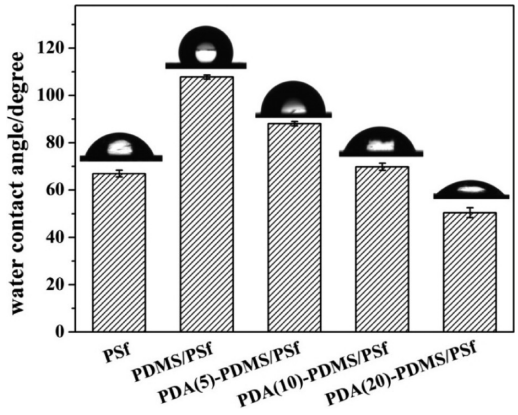

Figure 6. Static water contact angle of the PSf, PDMS/PSf, and PDA−PDMS/PSf supports for TFC membranes. Test temperature: 298 K.

3.3. Separation Performances of PDA−PDMS/PSf Supports. The gas transport behavior of the PDA−PDMS/PSf supports was investigated using pure gas (CO_2 and N_2) measurement. For comparison, the pristine PDMS/PSf support was the control membrane. Figure 7 shows the separation performances of the PDMS/PSf and PDA−PDMS/PSf supports with different PDA deposition time. The CO_2 permeance of the PDMS/PSf support increases slightly with increasing feed pressure, while N_2 reveals the opposite trend. Therefore, there is a slight increase in CO_2/N_2 ideal selectivity with increasing feed pressure for the PDMS/PSf support. These results are consistent with the previous study, demonstrating the formation of a defect-free dense PDMS layer on the PSf porous support.[46] With respect to the PDA−PDMS/PSf supports, as the deposition time increases, a growing amount of PDA is deposited to form PDA coating on the surface of the PDMS intermediate layer, which has been demonstrated in XPS analysis. Hence, the formed PDA layer could gradually become thicker over deposition time.[47] It is therefore obvious that not only the CO_2 permeance but also the N_2 permeance decreases with increasing PDA deposition time, which is attributed to the increased gas transport resistance. Never-

DOI: 10.1021/acsami.5b03786
ACS Appl. Mater. Interfaces 2015, 7, 15481−15493

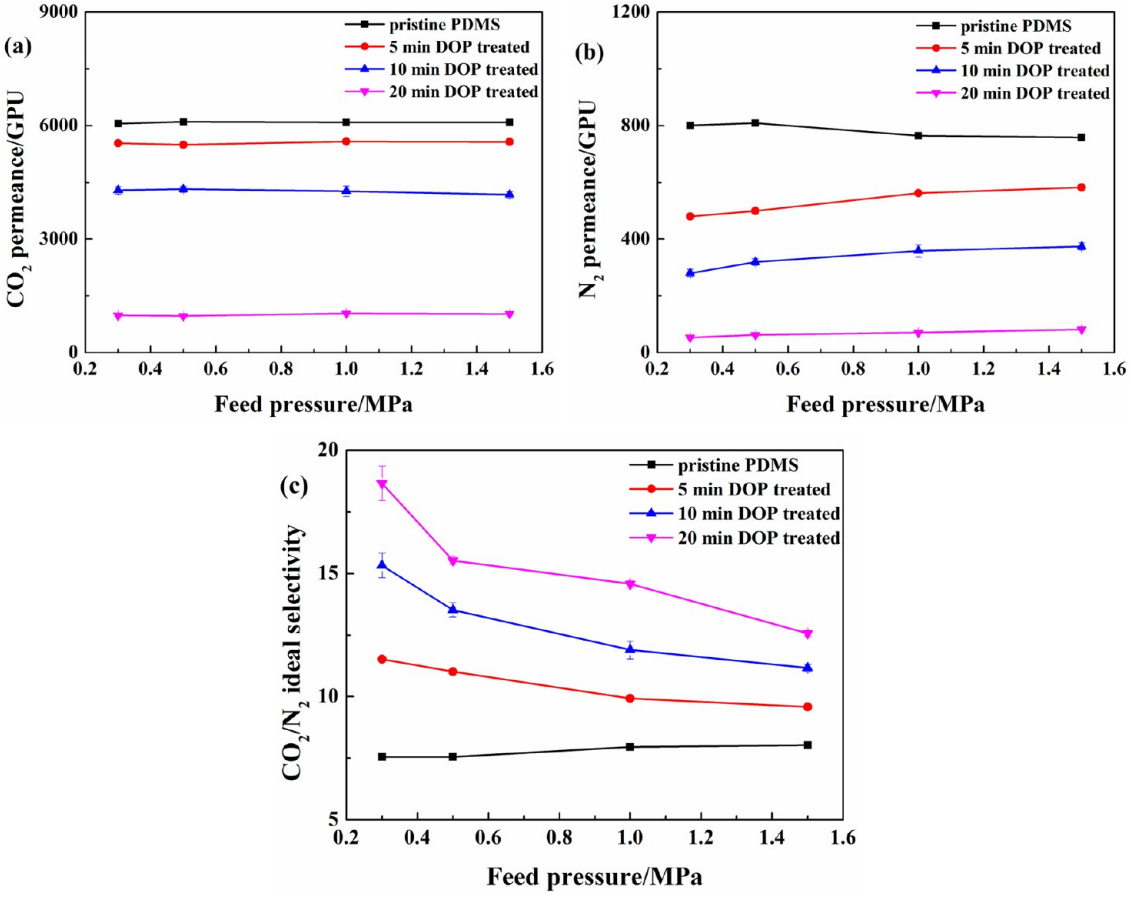

Figure 7. Effect of PDA deposition time on the separation performance of the PDA–PDMS/PSf supports: (a) CO_2 permeance, (b) N_2 permeance; (c) CO_2/N_2 ideal selectivity. Test temperature: 298 K. Test gas: Pure CO_2 and N_2 gas (>99.999 vol %).

theless, the CO_2/N_2 ideal selectivity displays the opposite trend owing to the increased content of introduced CO_2-philic functional groups from PDA. These polar functional groups could enhance CO_2 solubility, resulting in a delayed decrease in CO_2 permeance with increasing PDA deposition time compared to that of N_2. It should be noted that the N_2 permeance increases mildly with increasing feed pressure for all cases, which implies that the formed PDA layers might be not strictly dense. Indeed, the formation of a pinhole-free PDA layer on dense supports has been suggested to require the deposition time of at least an hour.[48] However, excess deposition time could result in a significant decrease in gas permeance accompanied by a very limited improvement of gas selectivity. In this work, the primary aim to construct a PDA layer is to tailor surface properties of the PDMS intermediate layer for benefiting the deposition of hydrophilic or even water-soluble CO_2-philic membrane materials, but not to develop a defect-free selective layer that is responsible for separation. Therefore, it is not necessary to prepare a fully dense PDA layer via enough deposition time of PDA at the expense of gas permeance.

3.4. Separation Performances of PVAm/PDA–PDMS/PSf Multilayer Composite Membranes. To investigate the influence of supports on the separation performance of TFC membranes, a series of TFC membranes based on various supports were developed, where the concentration of PVAm aqueous solution for selective layer was controlled at 1.0 wt %. Figure 8 illustrates the separation performance of different TFC membranes. The composite membrane based on the PSf

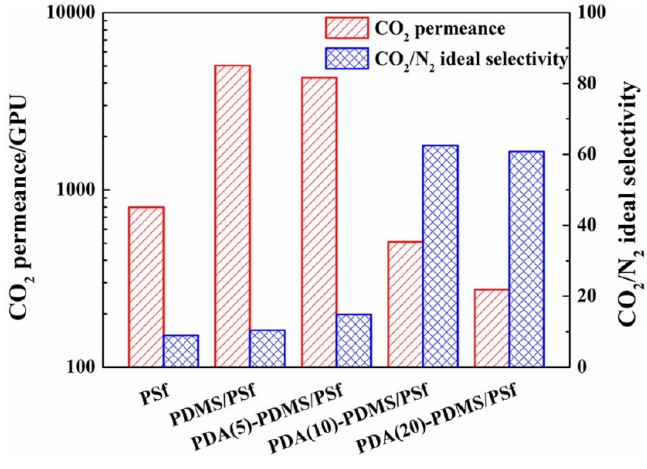

Figure 8. Effects of supports on the separation performance of TFC membranes. Coating solution: 1.0 wt % PVAm aqueous solution. Feed pressure: 0.30 MPa. Test gas: Pure CO_2 and N_2 gas (>99.999 vol %).

porous support exhibits an extremely low CO_2/N_2 ideal selectivity which is much lower than the reported value of about 64 from the membrane prepared using the PVAm concentration of 2.0 wt %.[39] This result implies that there may exist some defects or pinholes in the selective layer of the PVAm(1.0)/PSf membrane. To get a further insight into the gas transport behavior of the PVAm(1.0)/PSf membrane, effect of feed pressure on N_2 permeance in pure N_2 gas test was investigated. Obviously, the N_2 permeance approximately

DOI: 10.1021/acsami.5b03786
ACS Appl. Mater. Interfaces 2015, 7, 15481–15493

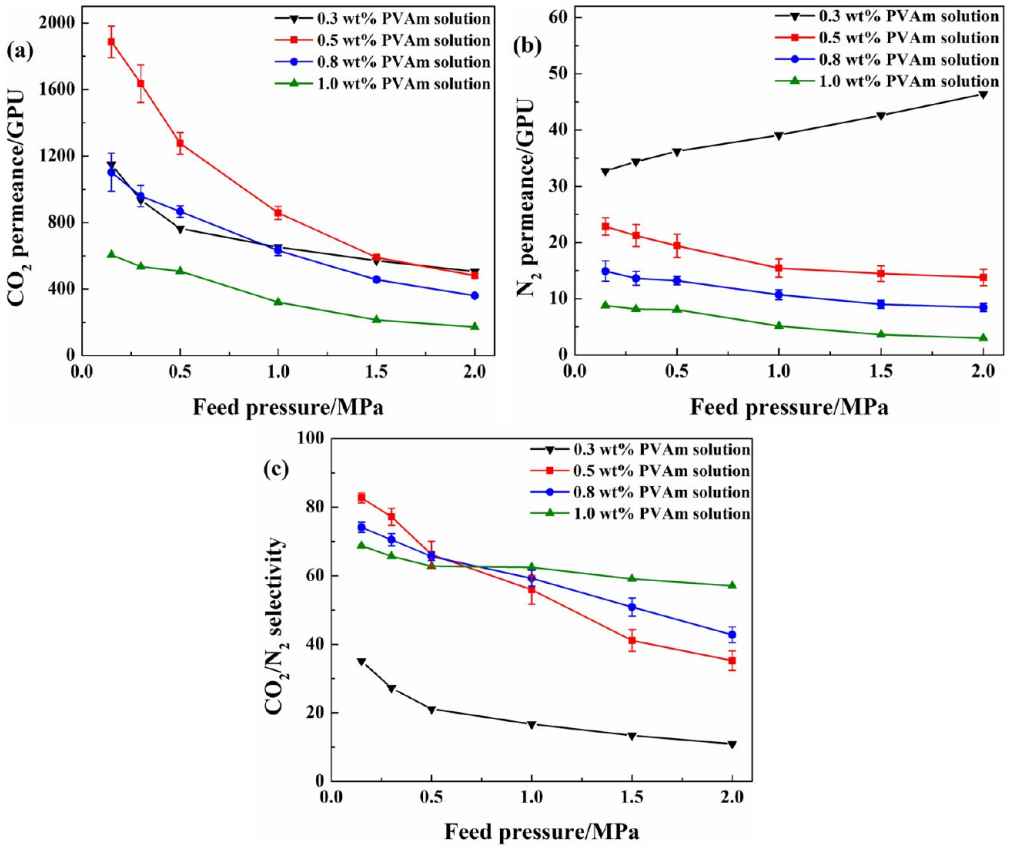

Figure 9. Effects of PVAm concentration on the separation performance of PVAm/PDA(10)-PDMS/PSf multilayer composite membranes: (a) CO_2 permeance, (b) N_2 permeance, and (c) CO_2/N_2 selectivity. Test gas: CO_2/N_2 mixed gas (15/85 by volume). Feed flow rate: 16 cm^3 (STP)/s. Sweep gas rate: 0.5 cm^3 (STP)/s.

increases linearly with increasing feed pressure in the pure N_2 gas test (Figure S7 in Supporting Information), which could be attributed to that the majority of gas molecules permeate through the membrane based on the Poiseuille flow mechanism.[49] This result further demonstrates the presence of defects in the selective layer. Therefore, it could be concluded that it is tough to develop a thin defect-free PVAm selective layer via directly coating the dilute PVAm aqueous solution onto the commercial PSf porous support, because pore penetration phenomenon could probably hinder perfect coverage of selective layer on porous support. Accordingly, introduction of a dense intermediate layer to prevent selective layer solution from penetration is essential for the fabrication of high-performance TFC membranes possessing a thin defect-free selective layer, especially when the coating solution with a relatively low concentration is used. It should be noted that the line scanning of cross section of composite membrane is usually an effective alternative method to determine whether pore penetration phenomenon occurs or not.[50] However, the thickness of every layer of the developed multilayer composite membranes is too small considering the resolution of energy-dispersive X-ray spectroscopy (EDX) associated with FESEM, hence the cross-sectional compositional change of composite membrane could not be accurately detected by EDX.[51] Therefore, pore penetration phenomenon was demonstrated via gas permeation experiment in this work.

Although pore penetration phenomenon is inhibited with regard to the PVAm(1.0)/PDMS/PSf and PVAm(1.0)/PDA(5)-PDMS/PSf membranes, both of them display the poor CO_2/N_2 ideal selectivity which is only slightly higher than that of the corresponding supports, suggesting that the formed PVAm selective layer is imperfect. Indeed, it is difficult to uniformly spread PVAm aqueous solution over the surfaces of the PDMS/PSf and PDA(5)-PDMS/PSf supports, which could be easily distinguished by the naked eyes. This phenomenon is caused by the hydrophobic nature of PDMS for the PDMS/PSf support characterized by high water contact angle. As for the PDA(5)-PDMS/PSf support, it is likely because that the limited deposited PDA within 5 min gives rise to a minor change in surface properties compared to the pristine PDMS/PSf support. The relative study has suggested that PDA deposition time of 10 min from a basic stirred solution was necessary for obtaining a topologically continuous PDA layer on the smooth supports without pores.[48] As a result, the PDMS/PSf and PDA(5)-PDMS/PSf supports could not be completely coated by PVAm aqueous solution. In sharp contrast, the CO_2/N_2 ideal selectivities of the PVAm(1.0)/PDA(10)-PDMS/PSf and PVAm(1.0)/PDA(20)-PDMS/PSf membranes are both similar to that of the reported PVAm(2.0)/PSf membrane, indicating the formation of a defect-free PVAm selective layer. In the light of general demand of high permeance for intermediate layer, the preferred PDA deposition time is 10 min in this work, since the PDA(10)-PDMS/PSf support possesses a much higher gas permeance than the PDA(20)-PDMS/PSf support. Therefore, the PDA(10)-PDMS/PSf support was selected as a suitable support of TFC membranes in the following.

As mentioned above, the selective layer of TFC membranes should be as thin as possible to achieve a high gas permeance,

DOI: 10.1021/acsami.5b03786
ACS Appl. Mater. Interfaces 2015, 7, 15481−15493

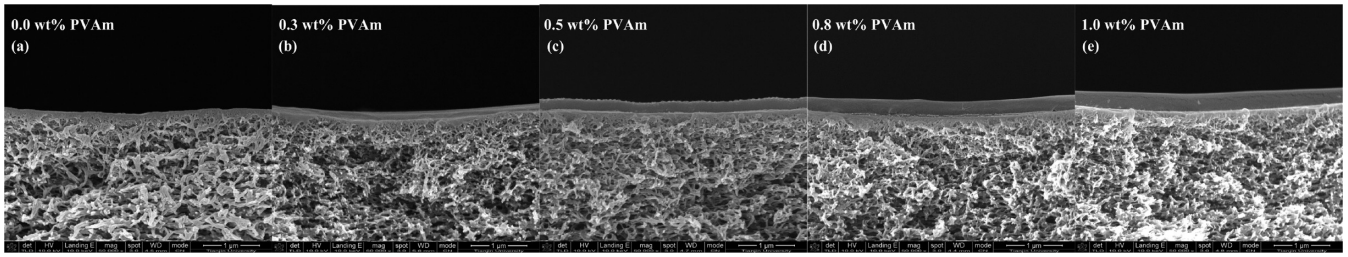

Figure 10. Cross-section SEM images of different membranes: (a) no PVAm coating, (b) 0.3 wt % PVAm, (c) 0.5 wt % PVAm, (d) 0.8 wt % PVAm, and (e) 1.0 wt % PVAm. Scale bar: 1 μm.

because it generally contributes most to the total gas transport resistance. The pore penetration phenomenon has been satisfactorily avoided after introducing the PDA-decorated PDMS intermediate layer. Therefore, the concentration of coating solutions could be further decreased to obtain a thinner selective layer. However, the coating solution with too low concentration could occasionally result in a defective layer caused by the unfavorable dewetting process that a thin liquid film is ruptured on the support.[17] This is probably due to the high mobility of polymer chains as a result of the lack of enough entanglement in the diluted solution.[52] For a specific support and polymer, a continuous liquid film forms on the support only above a critical polymer solution concentration.[53] Thus, the optimum PVAm concentration of coating solution should be explored considering both permeance and selectivity. Figure 9 presents the separation performance of TFC membranes with different PVAm concentrations. These membranes all display the typical facilitated transport behavior besides the PVAm(0.3)/PDA(10)−PDMS/PSf membrane. The CO_2 permeance drops with increasing feed pressure especially at the low feed pressure, because of carrier approaching saturation phenomenon.[36] A decreasing number of amino groups are available to interact with CO_2 molecules with increasing feed pressure. Hence, an increasing number of CO_2 molecules permeate through the membrane based on the solution-diffusion mechanism instead of the facilitated transport mechanism, resulting in an obvious decrease in CO_2 permeance with increasing feed pressure. Meanwhile the N_2 permeance decreases mainly because of salting-out effects. The increased salting concentration caused by the reaction between CO_2 and amino group, results in the decreased N_2 solubility and consequently the decreased N_2 permeance.[54] With respect to the influence of PVAm concentration, a notable increase in gas permeance is expectedly observed with decreasing PVAm concentration within the range of 0.5−1.0 wt %, which is primarily owing to the following two reasons. On one hand, a diluted coating solution concentration could result in a decreased selective layer thickness and consequently a reduced gas transport resistance. From SEM images of cross section structures of multilayer composite membranes (Figure 10), the PVAm selective layer thickness of different PVAm/PDA(10)-PDMS/PSf membranes with the PVAm concentrations of 1.0, 0.8, and 0.5 wt %, is about 309, 257, and 165 nm, respectively, namely the thickness of selective layers decreases with reducing coating solution concentration. On the other hand, when the thickness of selective layer declines toward the polymer radius of gyration, the chain mobility would be notably enhanced in the confined space, which could increase fractional free volume and consequently promote gas transport.[22] At the range of low feed pressure, the CO_2/N_2 selectivity increases with decreasing PVAm concentration, indicating a more significant increase in CO_2 permeance than N_2. This phenomenon is mainly owing to the more remarkable facilitated transport effect for a thinner facilitated transport selective layer.[55] Noteworthy is that not only the facilitated transport behavior but also the aforementioned change tendency of membrane performances with PVAm concentration is not observed for the PVAm(0.3)/PDA(10)−PDMS/PSf membrane, though it possesses the thinnest PVAm selective layer of about 103 nm from the cross-section image. Its CO_2/N_2 selectivity is much lower than that of the above membranes with relatively high PVAm concentrations, meanwhile, the N_2 permeance increases with increasing feed pressure even at the low feed pressure range, which both imply that the PVAm selective layer is not intact. It is likely caused by the dewetting phenomenon during solvent evaporation process, thus the generated defects influence and determine gas transport properties of TFC membrane. Overall, the PVAm(0.5)/PDA(10)−PDMS/PSf membrane displays the best performance that the CO_2 permeance of 1887 GPU with the CO_2/N_2 selectivity of 83 could be obtained at 0.15 MPa feed pressure. The CO_2/N_2 selectivity of the membrane with a thinner selective layer decreases more remarkably with increasing feed pressure, which is due to a more rapid decrease in CO_2 permeance caused by carrier approaching saturation.[36,55] Although there is an obvious decrease in CO_2/N_2 selectivity of the PVAm(0.5)/PDA(10)−PDMS/PSf membrane with increasing feed pressure, it could remain more than 35 at 2.0 MPa feed pressure. In addition, there is no obvious CO_2-induced plasticization phenomenon that could seriously deteriorate CO_2/N_2 selectivity. Therefore, diluting PVAm coating solution could significantly improve the gas permeance of TFC membranes while retaining the favorable gas selectivity after introducing the PDA-decorated PDMS intermediate layer.

3.5. Separation Performances of Pebax 1657/PDA−PDMS/PSf Multilayer Composite Membranes. In addition to amino groups containing polymers for facilitated transport membranes for CO_2 separation, another type of representative membrane materials for CO_2-philic polymeric membranes is ethylene oxide (EO) groups containing polymers which display a strong affinity toward CO_2 owing to the quadrupole−dipole interaction between CO_2 and EO group.[56] The most common EO groups containing polymers are commercial available PEO-based copolymers such as Pebax 1657.[8] Currently, the popular solvent for Pebax 1657 is the mixture of ethanol/water (70/30 wt %). It is not only an environmentally benign and economical solvent, but it could not destroy the structure of conventional polymeric supports for TFC membranes, which is a crucial advantage for fabricating composite membranes compared to other solvents. As anticipated, it is difficult for Pebax 1657 solution to spread homogeneously over the surface of the hydrophobic cross-linked PDMS intermediate layer when the

DOI: 10.1021/acsami.5b03786
ACS Appl. Mater. Interfaces 2015, 7, 15481−15493

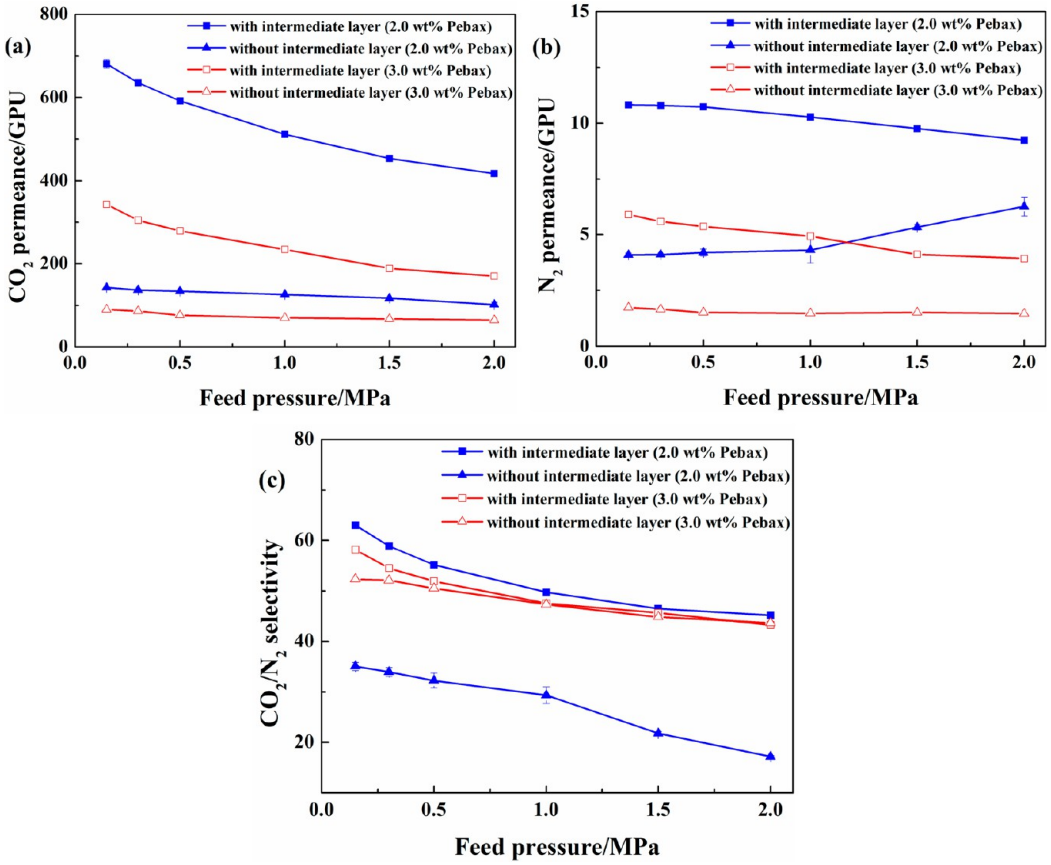

Figure 11. Comparison of Pebax 1657 composite membranes with and without PDA(10)-PDMS intermediate layer: (a) CO_2 permeance, (b) N_2 permeance, (c) CO_2/N_2 selectivity. Test gas: CO_2/N_2 mixed gas (15/85 by volume).

ethanol/water mixed solvent was used in this work. Fortunately, it could facilely spread and further firmly adhere on the surface of the as-developed PDA-decorated PDMS intermediate layer, which is probably attributed to hydrogen-bonding interactions between different polar groups of PDA and Pebax 1657.[57] Hence, CO_2-philic Pebax 1657/PDA(10)−PDMS/PSf multilayer composite membranes were successfully fabricated. Figure 11 depicts the separation performance of Pebax 1657-based composite membranes with and without the PDA-decorated PDMS intermediate layer. Different from in the facilitated transport PVAm selective layer introduced above, the transport of both gas molecules follows the solution-diffusion mechanism in the Pebax 1657 selective layer, thus both CO_2 permeance and CO_2/N_2 selectivity decrease slightly with the increment of feed pressure. Furthermore, the Pebax 1657/PDA(10)−PDMS/PSf membranes exhibit a significantly higher CO_2 permeance combined with a slightly higher CO_2/N_2 selectivity in comparison with the Pebax 1657/PSf membranes, especially the membranes prepared using the coating solution with the lower Pebax 1657 concentration. The CO_2 permeance of the Pebax 1657(2.0)/PDA(10)−PDMS/PSf membrane is 681 GPU at 0.15 MPa feed pressure, which is nearly five times that of the Pebax 1657(2.0)/PSf membrane. Meanwhile, the corresponding CO_2/N_2 selectivity (~63) is almost twice. It should be mentioned that the unfavorable CO_2 permeance and CO_2/N_2 selectivity of the Pebax 1657(2.0)/PSf membrane could be the consequence of pore penetration phenomenon which leads to a thick but still defective selective layer.[58] In summary, introduction of the PDA-decorated PDMS intermediate layer is also an efficient alternative approach for fabricating CO_2-philic polymeric membranes with improved performance.

3.6. Structural Stability of Multilayer Composite Membranes. The structural stability of the membrane is a vital issue from the view of practical application. Support and selective layer are generally made from different materials for a composite membrane. The swelling of hydrophobic support could possibility result in the detachment of hydrophilic selective layer from the support, and the swelling of hydrophilic selective layer could possibility lead to its detachment from the hydrophobic support as well, especially when the selective layer does not embed into the support.[59] With respect to the multilayer composite membranes described above, the hydrophobic cross-linked PDMS as intermediate layer could be swollen by organic solvents such as hexane, while the hydrophilic PVAm and Pebax 1657 as selective layer could be swollen by water.[39,60] Therefore, as an example, the structural stability of the PVAm(0.8)/PDA(10)−PDMS/PSf membrane was investigated. As shown in Figure 12, there is no obvious separation performance deterioration after hexane treatment, suggesting that PVAm selective layer is still immobilized on top of the intermediate layer, although the intermediate layer was swollen during the hexane treatment. Moreover, a 100-h continuous gas permeation test was conducted at 0.30 MPa feed pressure and 298 K, during which time the membrane was exposed to the humid atmosphere all the time. As illustrated in Figure 13, the membrane performance remains stable within the test period, indicating that the water-swollen PVAm selective layer still firmly adhere on the intermediate layer, even though there is no portion of PVAm selective layer that

DOI: 10.1021/acsami.5b03786
ACS Appl. Mater. Interfaces 2015, 7, 15481−15493

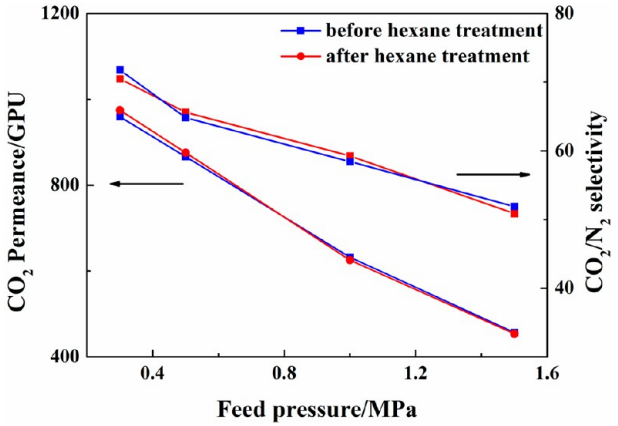

Figure 12. Effect of hexane treatment on the performance of the PVAm(0.8)/PDA(10)−PDMS/PSf multilayer composite membrane. Test gas: CO_2/N_2 mixed gas (15/85 by volume).

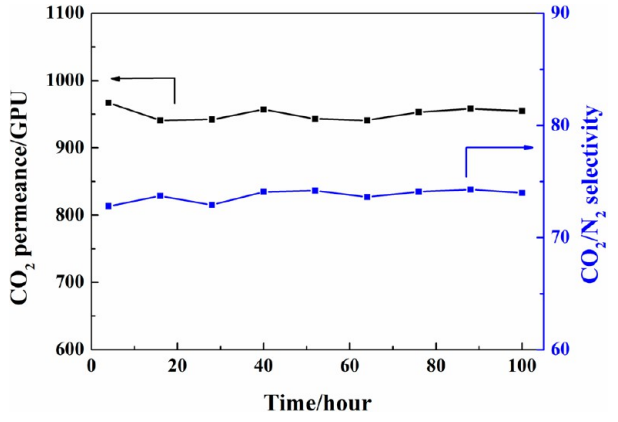

Figure 13. Stability of the PVAm(0.8)/PDA(10)−PDMS/PSf multilayer composite membrane for up to 100 h. Test gas: CO_2/N_2 mixed gas (15/85 by volume). Feed pressure: 0.30 MPa.

embeds in the intermediate layer. These results arise from multiple interactions (hydrogen bond, ionic bond and covalent bond) between PDA layer and PVAm layer. These bonding mechanisms have been demonstrated by ATR-FTIR, XPS and Raman analysis. Moreover, the hydrogen bond interaction between PDMS layer and PDA layer verified by ATR-FTIR study provides the favorable structural stability combined with the intrinsic strong adhesive property of PDA.[33] In addition, the partial intrusion of PDMS layer into PSf porous support ensures the good stability between PDMS layer and PSf porous support (Scheme 1), resembling that of conventional composite membranes such as reverse osmosis membrane. Therefore, an excellent structural stability of the developed multilayer composite membranes was achieved.

As introduced above, enhanced CO_2 separation performances of the facilitated transport membrane with a PVAm selective layer and the CO_2-philic polymeric membrane with a Pebax 1657 selective layer, are achieved with the help of PDA-decorated PDMS intermediate layer. Following this strategy, higher performance membranes are expected via incorporating various amino group-rich and EO group-rich low-molecular-weight additives into PVAm and Pebax 1657 selective layers, respectively.[36,61,62] Moreover, the codeposition of DOP and polyethylenimine (PEI) on the PDMS intermediate layer may further improve CO_2 separation performance owing to increased amino group content from PEI.[63] In addition, the optimization of PDMS coating method via prewetting porous support will further reduce the transport resistance of the intermediate layer, and consequently promote gas transport.[19]

4. CONCLUSION

In this work, the multilayer composite membranes with a significantly enhanced CO_2 separation performance were developed following a facile strategy of introducing a versatile molecular bridge between the hydrophobic PDMS intermediate layer and the hydrophilic PVAm selective layer, which could be readily achieved via surface modification of the intermediate layer using highly hydrophilic and adhesive PDA prior to selective layer deposition. Benefited from the formation of an ultrathin defect-free PVAm selective layer on the PDA-decorated PDMS intermediate layer, the resulting membranes display an excellent CO_2 permeance with a favorable CO_2/N_2 selectivity, which is promising for postcombustion CO_2 capture. Moreover, the superior structural stability of the developed multilayer composite membranes is ensured owing to the strong adhesion of PDA on PDMS intermediate layer and multiple (noncovalent and covalent) interactions between PDA and PVAm selective layer. In addition, CO_2-philic PEO based multilayer composite membranes with the PDA-decorated PDMS intermediate layer were fabricated for enhanced performance as well. This work may provide a universal and efficient strategy toward high-performance multilayer composite membranes with hydrophilic selective layers coated on hydrophobic supports for various separation applications.

■ ASSOCIATED CONTENT

Supporting Information

Synthesis and characterization of PDA, PVAm, and PDA@PVAm complex and gas permeation apparatus and separation performance of PVAm/PSf membrane. The Supporting Information is available free of charge on the ACS Publications website at DOI: 10.1021/acsami.5b03786.

■ AUTHOR INFORMATION

Corresponding Author

*Fax: +86 22 2740 4496. Tel: +86 22 2740 4533. E-mail: wangzhi@tju.edu.cn.

Notes

The authors declare no competing financial interest.

■ ACKNOWLEDGMENTS

This work is supported by the National Natural Science Foundation of China (21436009), the National High Technology Research and Development Program of China (2012AA03A611) and Program of Introducing Talents of Discipline to Universities (B06006).

■ REFERENCES

(1) Gin, D. L.; Noble, R. D. Designing the Next Generation of Chemical Separation Membranes. *Science* **2011**, *332*, 674−676.

(2) Brunetti, A.; Scura, F.; Barbieri, G.; Drioli, E. Membrane Technologies for CO_2 Separation. *J. Membr. Sci.* **2010**, *359*, 115−125.

(3) Seoane, B.; Coronas, J.; Gascon, I.; Benavides, M. E.; Karvan, O.; Caro, J.; Kapteijn, F.; Gascon, J. Metal-Organic Framework Based Mixed Matrix Membranes: A Solution for Highly Efficient CO_2 Capture? *Chem. Soc. Rev.* **2015**, *44*, 2421−2454.

(4) Buonomenna, M. G. Membrane Processes for a Sustainable Industrial Growth. *RSC Adv.* **2013**, *3*, 5694−5740.

DOI: 10.1021/acsami.5b03786
ACS Appl. Mater. Interfaces 2015, 7, 15481−15493

(5) Bernardo, P.; Drioli, E.; Golemme, G. Membrane Gas Separation: A Review/State of the Art. *Ind. Eng. Chem. Res.* **2009**, *48*, 4638−4663.
(6) Li, S.; Wang, Z.; Yu, X.; Wang, J.; Wang, S. High-performance Membranes with Multi-permselectivity for CO_2 Separation. *Adv. Mater.* **2012**, *24*, 3196−3200.
(7) Liao, J.; Wang, Z.; Gao, C.; Li, S.; Qiao, Z.; Wang, M.; Zhao, S.; Xie, X.; Wang, J.; Wang, S. Fabrication of High-performance Facilitated Transport Membranes for CO_2 Separation. *Chem. Sci.* **2014**, *5*, 2843−2849.
(8) Li, Y.; Wang, S.; Wu, H.; Guo, R.; Liu, Y.; Jiang, Z.; Tian, Z.; Zhang, P.; Cao, X.; Wang, B. High-performance Composite Membrane with Enriched CO_2-philic Groups and Improved Adhesion at the Interface. *ACS Appl. Mater. Interfaces* **2014**, *6*, 6654−6663.
(9) Low, B. T.; Zhao, L.; Merkel, T. C.; Weber, M.; Stolten, D. A Parametric Study of the Impact of Membrane Materials and Process Operating Conditions on Carbon Capture from Humidified Flue Gas. *J. Membr. Sci.* **2013**, *431*, 139−155.
(10) Merkel, T. C.; Lin, H.; Wei, X.; Baker, R. Power Plant Post-combustion Carbon Dioxide Capture: An Opportunity for Membranes. *J. Membr. Sci.* **2010**, *359*, 126−139.
(11) Park, H. B.; Jung, C. H.; Lee, Y. M.; Hill, A. J.; Pas, S. J.; Mudie, S. T.; Van Wagner, E.; Freeman, B. D.; Cookson, D. J. Polymers with Cavities Tuned for Fast Selective Transport of Small Molecules and Ions. *Science* **2007**, *318*, 254−258.
(12) Guiver, M. D.; Lee, Y. M. Polymer Rigidity Improves Microporous Membranes. *Science* **2013**, *339*, 284−285.
(13) Peng, Y.; Li, Y.; Ban, Y.; Jin, H.; Jiao, W.; Liu, X.; Yang, W. Metal-Organic Framework Nanosheets as Building Blocks for Molecular Sieving Membranes. *Science* **2014**, *346*, 1356−1359.
(14) Baker, R. W.; Low, B. T. Gas Separation Membrane Materials: A Perspective. *Macromolecules* **2014**, *47*, 6999−7013.
(15) Kim, S.; Lee, Y. M. Rigid and Microporous Polymers for Gas Separation Membranes. *Prog. Polym. Sci.* **2015**, *43*, 1−32.
(16) Ramasubramanian, K.; Zhao, Y.; Winston Ho, W. S. CO_2 Capture and H_2 Purification: Prospects for CO_2-selective Membrane Processes. *AIChE J.* **2013**, *59*, 1033−1045.
(17) Yave, W.; Car, A.; Wind, J.; Peinemann, K. V. Nanometric Thin Film Membranes Manufactured on Square Meter Scale: Ultra-thin Films for CO_2 Capture. *Nanotechnology* **2010**, *21*, 395301.
(18) Henis, J. M. S.; Tripodi, M. K. Composite Hollow Fiber Membranes for Gas Separation: The Resistance Model Approach. *J. Membr. Sci.* **1981**, *8*, 233−246.
(19) Li, P.; Chen, H. Z.; Chung, T.-S. The Effects of Substrate Characteristics and Pre-Wetting Agents on PAN−PDMS Composite Hollow Fiber Membranes for CO_2/N_2 and O_2/N_2 Separation. *J. Membr. Sci.* **2013**, *434*, 18−25.
(20) Gurr, P. A.; Scofield, J. M. P.; Kim, J.; Fu, Q.; Kentish, S. E.; Qiao, G. G. Polyimide Polydimethylsiloxane Triblock Copolymers for Thin Film Composite Gas Separation Membranes. *J. Polym. Sci., Part A: Polym. Chem.* **2014**, *52*, 3372−3382.
(21) Peter, J.; Peinemann, K. V. Multilayer Composite Membranes for Gas Separation Based on Crosslinked PTMSP Gutter Layer and Partially Crosslinked Matrimid® 5218 Selective Layer. *J. Membr. Sci.* **2009**, *340*, 62−72.
(22) Yave, W.; Huth, H.; Car, A.; Schick, C. Peculiarity of a CO_2-philic Block Copolymer Confined in Thin Films with Constrained Thickness: "A Super Membrane for CO_2-Capture". *Energy Environ. Sci.* **2011**, *4*, 4656−4661.
(23) Wang, M.; Wang, Z.; Li, S.; Zhang, C.; Wang, J.; Wang, S. A High Performance Antioxidative and Acid Resistant Membrane Prepared by Interfacial Polymerization for CO_2 Separation from Flue Gas. *Energy Environ. Sci.* **2013**, *6*, 539−551.
(24) Chen, H. Z.; Thong, Z.; Li, P.; Chung, T.-S. High Performance Composite Hollow Fiber Membranes for CO_2/H_2 and CO_2/N_2 Separation. *Int. J. Hydrogen Energy* **2014**, *39*, 5043−5053.
(25) Lin, H.; He, Z.; Sun, Z.; Vu, J.; Ng, A.; Mohammed, M.; Kniep, J.; Merkel, T. C.; Wu, T.; Lambrecht, R. C. CO_2-selective Membranes for Hydrogen Production and CO_2 Capture − Part I: Membrane Development. *J. Membr. Sci.* **2014**, *457*, 149−161.
(26) Morent, R.; De Geyter, N.; Axisa, F.; De Smet, N.; Gengembre, L.; De Leersnyder, E.; Leys, C.; Vanfleteren, J.; Rymarczyk-Machal, M.; Schacht, E.; Payen, E. Adhesion Enhancement by a Dielectric Barrier Discharge of Pdms Used for Flexible and Stretchable Electronics. *J. Phys. D: Appl. Phys.* **2007**, *40*, 7392.
(27) Lee, H.; Dellatore, S. M.; Miller, W. M.; Messersmith, P. B. Mussel-inspired Surface Chemistry for Multifunctional Coatings. *Science* **2007**, *318*, 426−430.
(28) Yang, H.-C.; Luo, J.; Lv, Y.; Shen, P.; Xu, Z.-K. Surface Engineering of Polymer Membranes via Mussel-inspired Chemistry. *J. Membr. Sci.* **2015**, *483*, 42−59.
(29) Kang, S. M.; You, I.; Cho, W. K.; Shon, H. K.; Lee, T. G.; Choi, I. S.; Karp, J. M.; Lee, H. One-step Modification of Superhydrophobic Surfaces by a Mussel-inspired Polymer Coating. *Angew. Chem., Int. Ed.* **2010**, *49*, 9401−9404.
(30) Thakur, V. K.; Vennerberg, D.; Kessler, M. R. Green Aqueous Surface Modification of Polypropylene for Novel Polymer Nanocomposites. *ACS Appl. Mater. Interfaces* **2014**, *6*, 9349−9356.
(31) Liu, Q.; Wang, N.; Caro, J.; Huang, A. Bio-inspired Polydopamine: A Versatile and Powerful Platform for Covalent Synthesis of Molecular Sieve Membranes. *J. Am. Chem. Soc.* **2013**, *135*, 17679−17682.
(32) Cao, Y.; Zhang, X.; Tao, L.; Li, K.; Xue, Z.; Feng, L.; Wei, Y. Mussel-inspired Chemistry and Michael Addition Reaction for Efficient Oil/Water Separation. *ACS Appl. Mater. Interfaces* **2013**, *5*, 4438−4442.
(33) Akter, T.; Kim, W. S. Reversibly Stretchable Transparent Conductive Coatings of Spray-deposited Silver Nanowires. *ACS Appl. Mater. Interfaces* **2012**, *4*, 1855−1859.
(34) Liu, Y.; Ai, K.; Lu, L. Polydopamine and Its Derivative Materials: Synthesis and Promising Applications in Energy, Environmental, and Biomedical Fields. *Chem. Rev.* **2014**, *114*, 5057−5115.
(35) Yu, B.; Liu, J.; Liu, S.; Zhou, F. Pdop Layer Exhibiting Zwitterionicity: A Simple Electrochemical Interface for Governing Ion Permeability. *Chem. Commun.* **2010**, *46*, 5900−5902.
(36) Qiao, Z.; Wang, Z.; Zhang, C.; Yuan, S.; Zhu, Y.; Wang, J.; Wang, S. PVAm−PIP/PS Composite Membrane with High Performance for CO_2/N_2 Separation. *AIChE J.* **2013**, *59*, 215−228.
(37) Zhao, S.; Wang, Z.; Wei, X.; Zhao, B.; Wang, J.; Yang, S.; Wang, S. Performance Improvement of Polysulfone Ultrafiltration Membrane Using PANiEB as Both Pore Forming Agent and Hydrophilic Modifier. *J. Membr. Sci.* **2011**, *385−386*, 251−262.
(38) Yu, X.; Wang, Z.; Wei, Z.; Yuan, S.; Zhao, J.; Wang, J.; Wang, S. Novel Tertiary Amino Containing Thin Film Composite Membranes Prepared by Interfacial Polymerization for CO_2 Capture. *J. Membr. Sci.* **2010**, *362*, 265−278.
(39) Li, P.; Wang, Z.; Liu, Y.; Zhao, S.; Wang, J.; Wang, S. A Synergistic Strategy via the Combination of Multiple Functional Groups into Membranes Towards Superior CO_2 Separation Performances. *J. Membr. Sci.* **2015**, *476*, 243−255.
(40) Islam, M. S.; Choi, W. S.; Lee, H.-J. Controlled Etching of Internal and External Structures of SiO_2 Nanoparticles Using Hydrogen Bond of Polyelectrolytes. *ACS Appl. Mater. Interfaces* **2014**, *6*, 9563−9571.
(41) Yuan, F.; Wang, Z.; Li, S.; Wang, J.; Wang, S. Formation−structure−performance Correlation of Thin Film Composite Membranes Prepared by Interfacial Polymerization for Gas Separation. *J. Membr. Sci.* **2012**, *421−422*, 327−341.
(42) Jiang, J.; Zhu, L.; Zhu, L.; Zhu, B.; Xu, Y. Surface Characteristics of a Self-polymerized Dopamine Coating Deposited on Hydrophobic Polymer Films. *Langmuir* **2011**, *27*, 14180−14187.
(43) Li, Y.; Su, Y.; Zhao, X.; He, X.; Zhang, R.; Zhao, J.; Fan, X.; Jiang, Z. Antifouling, High-flux Nanofiltration Membranes Enabled by Dual Functional Polydopamine. *ACS Appl. Mater. Interfaces* **2014**, *6*, 5548−5557.
(44) Das, J. K.; Das, N.; Bandyopadhyay, S. Highly Selective SAPO 34 Membrane on Surface Modified Clay−alumina Tubular Support for H_2/CO_2 Separation. *Int. J. Hydrogen Energy* **2012**, *37*, 10354−10364.

DOI: 10.1021/acsami.5b03786
ACS Appl. Mater. Interfaces 2015, 7, 15481−15493

(45) Liu, G.; Hung, W.-S.; Shen, J.; Li, Q.; Huang, Y.-H.; Jin, W.; Lee, K.-R.; Lai, J.-Y. Mixed Matrix Membranes with Molecular-interaction-driven Tunable Free Volumes for Efficient Bio-fuel Recovery. *J. Mater. Chem. A* **2015**, *3*, 4510−4521.
(46) Merkel, T. C.; Bondar, V. I.; Nagai, K.; Freeman, B. D.; Pinnau, I. Gas Sorption, Diffusion, and Permeation in Poly(dimethylsiloxane). *J. Polym. Sci., Part B: Polym. Phys.* **2000**, *38*, 415−434.
(47) Li, B.; Liu, W.; Jiang, Z.; Dong, X.; Wang, B.; Zhong, Y. Ultrathin and Stable Active Layer of Dense Composite Membrane Enabled by Poly(dopamine). *Langmuir* **2009**, *25*, 7368−7374.
(48) Zangmeister, R. A.; Morris, T. A.; Tarlov, M. J. Characterization of Polydopamine Thin Films Deposited at Short Times by Autoxidation of Dopamine. *Langmuir* **2013**, *29*, 8619−8628.
(49) Li, S.; Wang, Z.; Zhang, C.; Wang, M.; Yuan, F.; Wang, J.; Wang, S. Interfacially Polymerized Thin Film Composite Membranes Containing Ethylene Oxide Groups for CO_2 Separation. *J. Membr. Sci.* **2013**, *436*, 121−131.
(50) Das, J. K.; Das, N. Mercaptoundecanoic Acid Capped Palladium Nanoparticles in a SAPO 34 Membrane: A Solution for Enhancement of H_2/CO_2 Separation Efficiency. *ACS Appl. Mater. Interfaces* **2014**, *6*, 20717−20728.
(51) Unger, W. S.; Hodoroaba, V.-D. Surface Chemical Analysis at the Micro- and Nanoscale. In *Handbook of Technical Diagnostics*; Czichos, H., Ed.; Springer: Berlin, 2013; Chapter 15, pp 301−322.
(52) Bonn, D.; Eggers, J.; Indekeu, J.; Meunier, J.; Rolley, E. Wetting and Spreading. *Rev. Mod. Phys.* **2009**, *81*, 739−805.
(53) Roy, S.; Ansari, K. J.; Jampa, S. S. K.; Vutukuri, P.; Mukherjee, R. Influence of Substrate Wettability on the Morphology of Thin Polymer Films Spin-coated on Topographically Patterned Substrates. *ACS Appl. Mater. Interfaces* **2012**, *4*, 1887−1896.
(54) He, W.; Wang, Z.; Li, W.; Li, S.; Bai, Z.; Wang, J.; Wang, S. Cyclic Tertiary Amino Group Containing Fixed Carrier Membranes for CO_2 Separation. *J. Membr. Sci.* **2015**, *476*, 171−181.
(55) Zhang, C.; Wang, Z.; Cai, Y.; Yi, C.; Yang, D.; Yuan, S. Investigation of Gas Permeation Behavior in Facilitated Transport Membranes: Relationship between Gas Permeance and Partial Pressure. *Chem. Eng. J.* **2013**, *225*, 744−751.
(56) Liu, S. L.; Shao, L.; Chua, M. L.; Lau, C. H.; Wang, H.; Quan, S. Recent Progress in the Design of Advanced PEO-Containing Membranes for CO_2 Removal. *Prog. Polym. Sci.* **2013**, *38*, 1089−1120.
(57) Li, Y.; Wang, S.; Wu, H.; Wang, J.; Jiang, Z. Bioadhesion-inspired Polymer-inorganic Nanohybrid Membranes with Enhanced CO_2 Capture Properties. *J. Mater. Chem.* **2012**, *22*, 19617−19620.
(58) Ren, X.; Ren, J.; Li, H.; Feng, S.; Deng, M. Poly (amide-6-b-ethylene oxide) Multilayer Composite Membrane for Carbon Dioxide Separation. *Int. J. Greenhouse Gas Control* **2012**, *8*, 111−120.
(59) Peng, J.; Su, Y.; Chen, W.; Zhao, X.; Jiang, Z.; Dong, Y.; Zhang, Y.; Liu, J.; Cao, X. Polyamide Nanofiltration Membrane with High Separation Performance Prepared by EDC/NHS Mediated Interfacial Polymerization. *J. Membr. Sci.* **2013**, *427*, 92−100.
(60) Ogieglo, W.; van der Werf, H.; Tempelman, K.; Wormeester, H.; Wessling, M.; Nijmeijer, A.; Benes, N. E. N-hexane Induced Swelling of Thin PDMS Films under Non-equilibrium Nanofiltration Permeation Conditions, Resolved by Spectroscopic Ellipsometry. *J. Membr. Sci.* **2013**, *431*, 233−243.
(61) Yave, W.; Car, A.; Funari, S. S.; Nunes, S. P.; Peinemann, K. V. CO_2-philic Polymer Membrane with Extremely High Separation Performance. *Macromolecules* **2010**, *43*, 326−333.
(62) Reijerkerk, S. R.; Wessling, M.; Nijmeijer, K. Pushing the Limits of Block Copolymer Membranes for CO_2 Separation. *J. Membr. Sci.* **2011**, *378*, 479−484.
(63) Yang, H.-C.; Pi, J.-K.; Liao, K.-J.; Huang, H.; Wu, Q.-Y.; Huang, X.-J.; Xu, Z.-K. Silica-decorated Polypropylene Microfiltration Membranes with a Mussel-Inspired Intermediate Layer for Oil-in-Water Emulsion Separation. *ACS Appl. Mater. Interfaces* **2014**, *6*, 12566−12572.

DOI: 10.1021/acsami.5b03786
ACS Appl. Mater. Interfaces 2015, 7, 15481−15493